IEEE Photonics Journal
An IEEE Photonics Society Publication

Open Access

Generation of High-Power Bottle Beams and Autofocusing Beams

Volume 10, Number 1, February 2018

Yixian Qian
Songtao Lai
Hongxing Mao

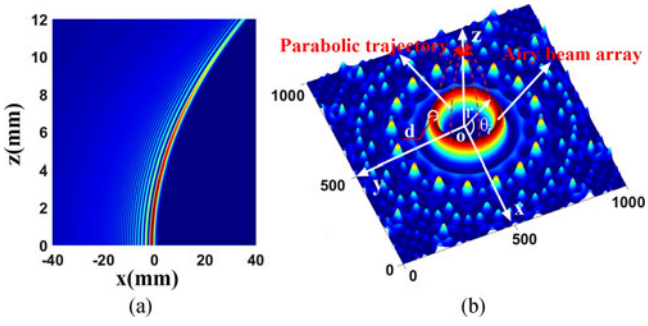

DOI: 10.1109/JPHOT.2018.2799165
1943-0655 © 2018 IEEE

Generation of High-Power Bottle Beams and Autofocusing Beams

Yixian Qian, Songtao Lai, and Hongxing Mao

Key Laboratory of Optical Information Detecting and Display Technology, Zhejiang Normal University, Jinhua 321004, China

DOI:10.1109/JPHOT.2018.2799165

Manuscript received December 5, 2017; revised January 22, 2018; accepted January 24, 2018. Date of publication January 30, 2018; date of current version February 21, 2018. This work was supported in part by the National Natural Science Foundation of China under Grant 61377014 and in part by the Zhejiang Provincial Natural Science Foundation under Grant LY17A040002. Corresponding author: Yixian Qian (e-mail: qianyixian@zjnu.edu.cn).

Abstract: We propose and experimentally demonstrate an optical bottle beam (BB) and an abruptly autofocusing beam (AB), which were generated using a ring-Airy beam array. The method can form BB arrays with varying sizes during propagation; consequently, it can produce multiple optical traps. Additionally, the BB size and the AB focal position can be controlled by varying the array radius. The intensity of the resulting beams improved significantly with increasing array number, and the value abruptly increased 800 times at the focal position when array radius and number were 2 mm and 64, respectively. It is the lateral acceleration of Airy beams that causes this abrupt increase in intensity. Numerical simulations were consistent with experimental results. These advantages could be beneficial for potential applications, such as optical traps, laser ablation, and the ignition of nonlinear effect. (The caption of Graphic Abstract is generation of high-power BBs and ABs using a ring-Airy beam array.)

Index Terms: Beam propagation, physics optics, optical bottle beam, autofocusing beam, self-acceleration.

1. Introduction

Optical bottle beams (BBs) are characterized by low or null intensity channels surrounded by three-dimensional regions of higher intensity [1]. Such beams can be applied to optical tweezers [2] for confining transparent particles as well as cells, DNA, atoms, and molecules by utilizing gradient optical forces (or radiation pressure) [3], [4]. The so-called optical bottle was first proposed in 1970 and used to create an optical potential well [5]. Ever since, the development of BBs has attracted considerable attention, due to their unusual properties, which include high intensity gradients and dark hollow areas. A variety of methods have been proposed for generating these beams. For example, a single optical BB can be generated with Moiré techniques and used to trap and transport aerosols [6]. The superposition of Bessel beams has been utilized to generate an array of BBs using a specially-designed diffractive optical element [7]. Recently, a hologram optical bottle beam was reported which can manipulate particles along arbitrary paths [8]. In addition, ultrafast hollow Gaussian beams were proposed using a linear and nonlinear method with only two spiral phase plates [9].

Focusing beams have potential in a variety of applications, such as optical trapping [4], [10] and intense light bullet generation [11], [12]. As such, the focusing performance of these beams

is always an issue of great practical significance. Efremidis *et al*. proposed and demonstrated an abruptly autofocusing beam (AB) using a radially symmetric Airy intensity distribution [13], [14]. The intensity of these beams undergoes an abrupt increase near the focal point. This abrupt autofocusing property and lack of additional lenses imply ABs are especially suitable for biomedical treatment or laser ablation. Such focal spots can only be produced by dynamically tailoring vector Bessel-Gaussian beams through their beam parameters [15], this method can also generate optical BBs. An autofocusing beam was recently produced with periodic lattices [16]. Conical circular Airy beams with significantly reduced focal lengths have also been investigated [17]. Metasurfaces have been utilized to generate autofocusing beams without the need for Fourier transforms [18]. More recently, a circular Airy beam was made to exhibit a dual abrupt focus by imposing a quadratic phase on its spectrum [19].

Airy beams were first observed by Siviloglou *et al*. in 2007 [20] and have generated substantial research interest due to their self-accelerating properties [21]. They have advanced rapidly for applications to light bullets [22], optical clearing [4], and plasma guiding [23]. In this study, we generate an optical BB by employing the self-accelerating properties of Airy beams. We theoretically develop and experimentally validate an efficient and simple method for generating high-power and controllable optical BBs, as well as ABs, using ring-Airy beam array. The BB size and AB focal position can be readily controlled by varying the array radius, and this property may allow for more freedom in the manipulation of a cell or particle. This method can form BB arrays of varying sizes during propagation and can consequently generate multiple optical traps. Additionally, the intensity of such beams improves dramatically with increasing array number. These advantages will be beneficial for potential applications, such as optical trapping, laser ablation, and the ignition of nonlinear effects.

2. Theory

To demonstrate the propagation behavior of optical BBs and ABs, we first consider the paraxial diffraction equation which governs the propagation dynamics of the electric field envelope ϕ [20]:

$$i\frac{\partial \phi}{\partial z} + \frac{1}{2k}\frac{\partial^2 \phi}{\partial x^2} = 0. \tag{1}$$

Here, x represents the one-dimensional transverse coordinate, z is the propagation distance, and $k = 2\pi/\lambda$ is the wavenumber. Equation (1) has a finite-energy Airy solution obtained by introducing an exponentially decaying factor exp(as) [20]:

$$\phi(x, z) = Ai[x - (z/2)^2 + iaz]\exp[ax - (az^2/2) - i(z^3/12) + i(a^2 z/2) + i(xz/2)). \tag{2}$$

In this expression, $Ai(\cdot)$ denotes an Airy function and a is a small positive quantity which can suppress the infinite Airy tail, ensuring the physical realization of Airy beams. The main lobe of the Airy beam follows a parabolic trajectory in the x–z plane, which is represented by the term $x - (z/2)^2$ in (2). Fig. 1(a) depicts the accelerating propagation as a function of the distance z.

Fig. 1(b) demonstrates the use of a ring-Airy beam array for generating BBs. In this configuration, multiple Airy beams are evenly- distributed in a circle in the x-y plane. Consequently, their main lobes form an obvious energy circle which results in an optical bottle beam. In the figure, r denotes the radius of the energy circle (or array radius), and it also represents the distance of main lobe of Airy beam away from optical axis. d indicates the width of the main lobe. Such arranged Airy beams move towards the center because they propagate along parabolic paths and will thus generate a downsized BB. Finally, these main lobes simultaneously converge at a point and form an autofocusing beam. The initial BB generated by a ring-Airy beam array is given by:

$$\phi_n(x, y, z = 0) = \sum_{i=1}^{n} \phi_i(r, \theta_i, z = 0), \tag{3}$$

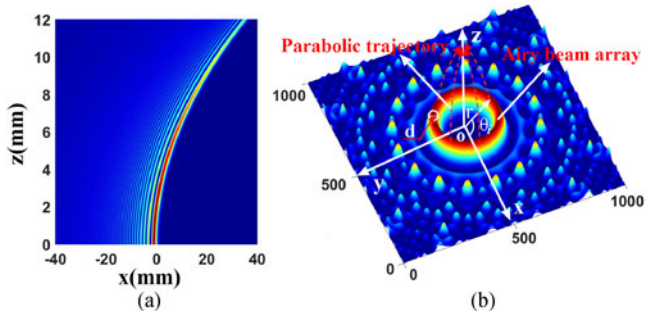

Fig. 1. (a) Propagation dynamics for a finite-energy Airy packet when $a = 0.01$. (b) Generation principles for an optical bottle beam.

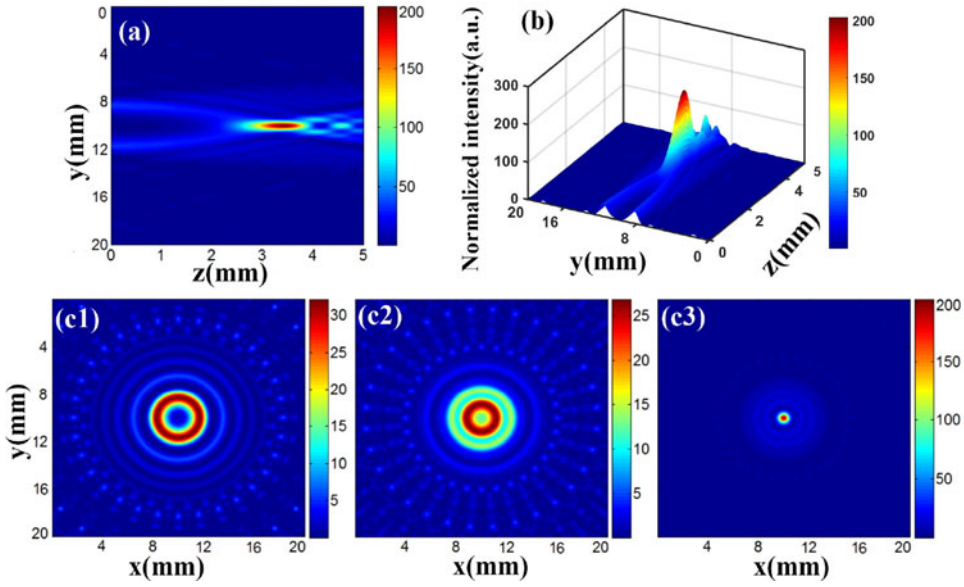

Fig. 2. The optical bottle beam and autofocusing beam. (a) The numerical side-view. (b) The normalized intensity. (c1)–(c3) Numerical intensity distributions at propagation distances of z $=$ 0, 1.8, and 3.3 mm, respectively, here the array number $n = 32$.

where ϕ_n is the initial BB optical field and n is the number of Airy beams (array number), ϕ_i denotes the ith Airy beam, and θ_i is the polar angle of the ith Airy beam. Here $r \cos \theta_i = x_i$ and $r \sin \theta_i = y_i$, where (x_i, y_i) is the location coordinate of the ith Airy beam in the $x - y$ plane. Under the paraxial approximation, the BB propagation obeys the Fresnel diffraction:

$$\phi_n(x, y, z) = \frac{\exp(ikz)}{i\lambda z} \iint \phi_n(x_0, y_0, 0) \exp\left[\frac{ik(x - x_0)^2 + (y - y_0)^2}{2z}\right] dx_0 dy_0, \tag{4}$$

where $\phi_n(x_0, y_0, 0)$ is the initial optical bottle beam. Fig. 2 displays the BB propagation dynamics for the case of $n = 32$. Fig. 2(a) and (b) demonstrate a numerical side-view and normalized intensity as a function of propagation distance, respectively. It is evident the Airy beams follow parabolic trajectories and converge to the same point, where intensity rapidly increases by a factor of 200 [Fig. 2(b)]. This abrupt increase in intensity is caused by lateral acceleration. Fig. 2(c1)–(c3) present numerical intensity distributions at propagation distances of z $=$ 0, 1.8, and 3.3 mm, respectively. The Airy beam arrays generate a hollow core [Fig. 2(c1)], which is surrounded by a high-intensity Airy-ring (main ring). Several subsequent Airy-rings are visible in the peripheral in simulations. The

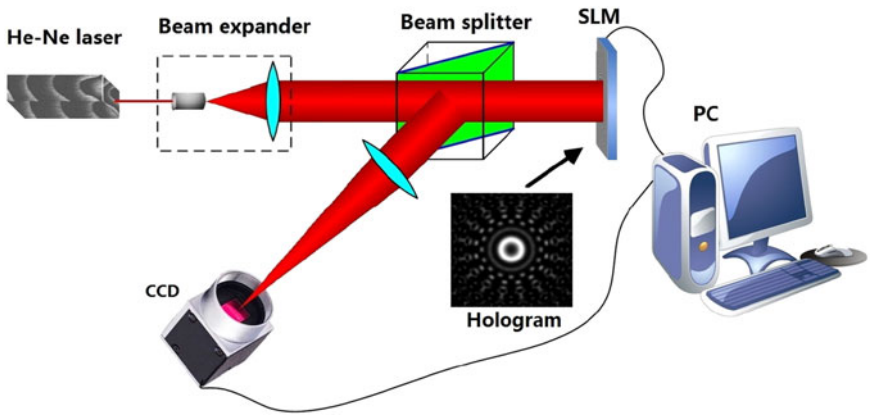

Fig. 3. Experimental setup.

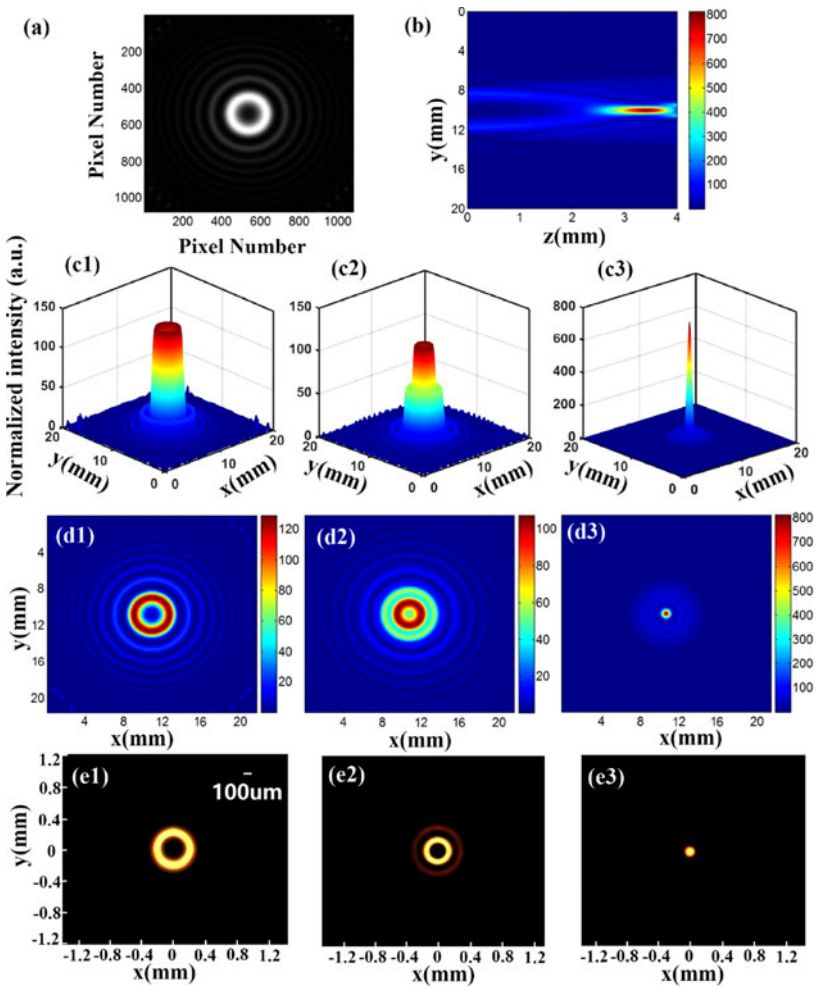

Fig. 4. The optical bottle beam and autofocusing beam. (a) The hologram. (b) The numerical side-view. (c1)–(c3) The 2D BB and AB. (d1)–(d3) Numerical intensity distributions for propagation distances of $z = 0$,1.8, and 3.3 mm, respectively. (e1)–(e3) The corresponding experimental results.

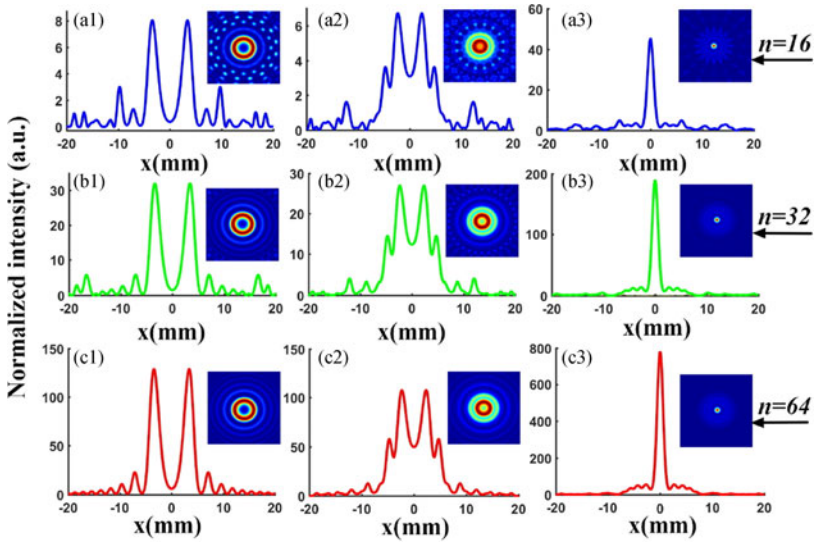

Fig. 5. A comparison of the normalized intensity profiles at z = 0, 1.8, and 3.3 mm. (a1)–(a3) $n = 16$, (b1)–(b3) $n = 32$, (c1)–(c3) $n = 64$. The insets display corresponding intensity distributions.

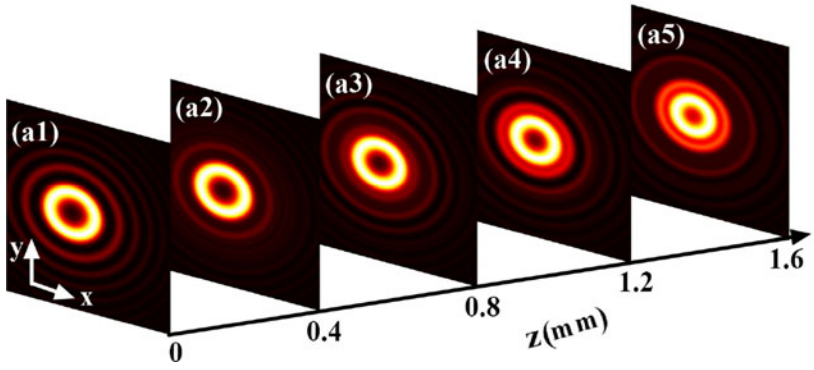

Fig. 6. An optical bottle array for varying propagation distance: (a1) z = 0, (a2) z = 0.4, (a3) z = 0.8, (a4) z = 1.2, and (a5) z = 1.6 mm, respectively. The array number $n = 64$ in each image.

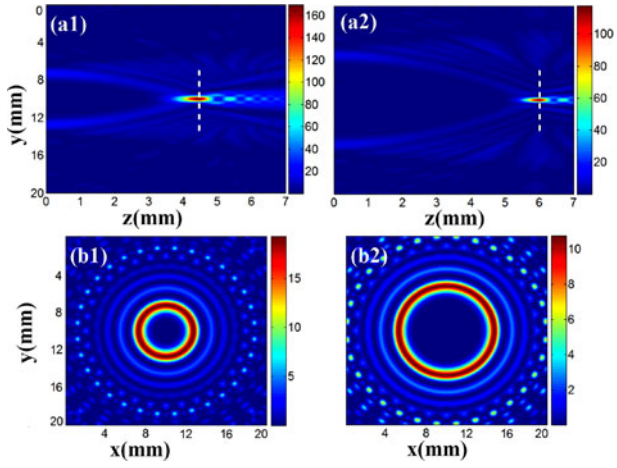

Fig. 7. A numerical side-view, (a1) $r = 4$ mm, and (a2) 8 mm. The images in (b1)–(b2) show corresponding intensity distributions in the initial plane for $n = 32$.

BB evolves into a focal point after propagating a distance of z = 3.3 mm. After this focal point, the maximum intensity gradually decreases. However, the decline is not monotonic but shows oscillations, as seen in Fig. 1(a). This phenomenon results from the interaction between the main Airy-ring and subsequent Airy-rings. The simulation assumed values of $r = 2$ mm, $d = 1$ mm, and $\lambda = 632.8 \times 10^{-6}$ mm.

3. Experimental Results

The optical BBs can also be generated by a phase-only reflecting spatial light modulator (SLM), as demonstrated in Fig. 3. The configuration is similar to that of previous studies [24]. The input He-Ne laser (632 nm) is employed to generate a collimated and expanded Gaussian beam with an 8.6 mm full-width-at-half-maximum (FWHM). The Gaussian beam is reflected by a computer-controlled SLM (resolution, 1920 × 1080 pixels; pixel size, 8 μm; Holoeye Pluto, HOLOEYE), which is imposed by a computer-generated hologram. And then, the phase-modulated and reflected beam undergo a Fourier transform through use of a Fourier lens with a focal length of $f' = 300$ mm. A BB can eventually be generated in the back focal plane of the Fourier lens, where the CCD can be moved along the optical axis to acquire snapshot images of the intensity profile. The SLM is located in the front focal plane of the Fourier lens.

Experimental parameters included an array number of $n = 64$ and other values similar to those of Fig. 2. Fig. 4(a) demonstrates the computer-generated hologram coded onto the SLM, which is the intensity interference pattern formed by Airy beam arrays and the plane wave. A numerical side-view of the BB is depicted in Fig. 4(b). Fig. 4(c1)–(c3) demonstrate a 2D high-power BB and an AB. Note the initial intensity is approximately 150 times larger than a single Airy beam due to multiple main lobes superposition. Subsequently, the BB tended to automatically focus without any auxiliary components or equipment. This results in an increase of as much as 800 times in the focal plane, with a focal spot diameter of approximately 100 μm. Due to the abrupt increase in intensity, the property would be beneficial for the ignition of nonlinear effects [12] and laser ablation [14]. Fig. 4(d1)–(d3) depict numerical intensity distributions at propagation distances of z = 0, 1.8, and 3.3 mm, respectively. The corresponding experimental results are shown in Fig. 4(e1)–(e3), respectively. These results are in good agreement with numerical simulations. Note that some of the peripheral Airy-rings disappear in the experimental beam, and the effect was caused by the use of a low-level laser. The optical conversion efficiency mainly depends on reflectivity and the diffraction loss caused by the pixel structure of SLM. The conversion efficiency is approximately 90% in our system.

Fig. 5 depicts a comparisons of normalized intensity profiles at distances of z = 0, 1.8, and 3.3 mm, for cases of $n = 16$, 32, and 64 in the first, second, and third lines of the figure, respectively. The inset images provide corresponding intensity distributions in x-y plane. As can be seen in Fig. 5(a1)–(c1), the high-power BB intensity improves significantly with an increasing array number. The normalized intensity was as much as 8 times larger than that of a single Airy beam when $n = 16$. However, this value increases to 150 times when $n = 64$ [see Fig. 5(c1)]. The intensity abruptly increases 800^{x} after propagating a distance of z = 3.3 mm [see Fig. 5(c3)]. There is an approximately null intensity region in the center of the initial intensity profile, surrounded by a high-intensity region. Such an optical field structure allows these beams to trap macroparticles.

The center region intensity remains null and invariable in the early propagation stages. However, the size of hollow core decreases during propagation. Consequently, optical bottle beam arrays are formed, as demonstrated in Fig. 6. This process clearly describes the evolution of optical BB arrays along the propagation direction. In contrast to traditional single optical bottle beams, optical bottle arrays simultaneously provide multiple trapping and manipulation.

In addition, we can readily control the BB size and focal position by varying the size of the array radius r. A larger value of r results in a longer focal length. Fig. 7(a1) and (a2) exhibit a controllable focal length in the case of $n = 32$, $r = 4$ mm and 8 mm, respectively. The focal length is approximately 6 mm when $r = 8$ mm mm. However, it is only 3.3 mm when $r = 2$ mm, as shown in Fig. 2(a). This also leads to a larger BB as depicted in Fig. 7(b1) and (b2), which correspond to

Fig. 7(a1) and (a2), respectively. This property may allow for more freedom in the manipulation of a cell or particle.

4. Conclusion

In summary, we have proposed and experimentally demonstrated an efficient method for generating high-power and controllable optical bottle beams, as well as autofocusing beams, by employing the self-accelerating properties of Airy beams. The BB size and focal length can be readily controlled by varying the array radius, this property would be beneficial for flexible optical manipulation. This method can also generate different sizes of BB arrays and form multiple optical traps. Furthermore, the intensity of such beams improves dramatically with increasing array number. These properties could be advantageous in a variety of medical applications or for the development of improved optical tweezers.

References

[1] J. Arlt and M. J. Padgett, "Generation of a beam with a dark focus surrounded by regions of higher intensity: The optical bottle beam," *Opt. Lett.*, vol. 25, no. 4, pp. 191–193, Mar. 2000.
[2] K. Dholakia, P. Reece, and M. Gu, "Optical micromanipulation," *Chem. Soc. Rev.*, vol. 37, no. 1, pp. 42–55, Feb. 2008.
[3] D. G. Grier, "A revolution in optical manipulation," *Nature*, vol. 424, no. 6950, pp. 810–816, Aug. 2003.
[4] J. Baumgartl, M. Mazilu, and K. Dholakia, "Optically mediated particle clearing using Airy wavepackets," *Nature Photon.*, vol. 2, no. 11, pp. 675–78, Nov. 2008.
[5] A. Ashkin, "Acceleration and trapping of particles by radiation pressure," *Phys. Rev. Lett.*, vol. 24, no. 4, pp. 156–159, Jan. 1970.
[6] P. Zhang *et al.*, "Trapping and transporting aerosols with a single optical bottle beam generated by moiré techniques," *Opt. Lett.*, vol. 36, no. 8, pp. 1491–1493, Apr. 2011.
[7] A. P. Porfirev and R. V. Skidanov, "Generation of an array of optical bottle beams using a superposition of Bessel beams," *Appl. Opt.*, vol. 52, no. 25, pp. 6230–6238, Sep. 2013.
[8] C. Alpmann, M. Esseling, P. Rose, and C. Denz, "Holographic optical bottle beams," *Appl. Phys. Lett.*, vol. 100, no. 11, Mar. 2012, Art. no. 111101.
[9] N. A. Chaitanya, A. Chaitanya, J. Banerji, and G. K. Samanta, "High power, higher order ultrafast hollow Gaussian beams," *Appl. Phys. Lett.*, vol. 110, no. 21, May 2017, Art. no. 211103.
[10] H. Cheng, W. Zang, W. Zhou, and J. Tian, "Analysis of optical trapping and propulsion of Rayleigh particles using Airy beam," *Opt. Exp.*, vol. 18, no. 19, pp. 20384–20394, Sep. 2010.
[11] D. Abdollahpour, S. Suntsov, D. G. Papazoglou, and S. Tzortzakis, "Spatiotemporal airy light bullets in the linear and nonlinear regimes," *Phys. Rev. Lett.*, vol. 105, no. 25, Dec. 2010, Art. no. 253901.
[12] P. Panagiotopoulos, D. G. Papazoglou, A. Couairon, and S. Tzortzakis, "Sharply autofocused ring-Airy beams transforming into non-linear intense light bullets," *Nature Commun.*, vol. 4, no. 4, Oct. 2013, Art. no. 2622.
[13] N. K. Efremidis and D. N. Christodoulides, "Abruptly autofocusing waves," *Opt. Lett.*, vol. 35, no. 23, pp. 4045–4047, Dec. 2010.
[14] D. G. Papazoglou, N. K. Efremidis, D. N. Christodoulides, and S. Tzortzakis, "Observation of abruptly autofocusing waves," *Opt. Lett.*, vol. 36, no. 10, pp. 1842–1844, May 2011.
[15] H. Ye *et al.*, "Intrinsically shaping the focal behavior with multi-ring Bessel-Gaussian beam," *Appl. Phys. Lett.*, vol. 111, no. 3, Jul. 2017, Art. no. 031103.
[16] P. Panagiotopoulos, D. G. Papazoglou, A. Couairon, and S. Tzortzakis, "Controlling high-power autofocusing waves with periodic lattices," *Opt. Lett.*, vol. 39, no. 16, pp. 4958–4961, Aug. 2014.
[17] J. Zhang, Y. Li, Z. Tian, and D. Lei, "Controllable autofocusing properties of conical circular Airy beams," *Opt.Commun.*, vol. 391, pp. 116–120, Jan. 2017.
[18] Q. Fan, D. Wang, P. Huo, T. Xu, Y. Liang, and Z. Zhang, "Autofocusing Airy beams generated by all-dielectric metasurface for visible light," *Opt. Exp.*, vol. 25, no. 8, pp. 9285–9294, Apr. 2017.
[19] J. Zhang and J. He, "Dual abruptly focus of modulated circular Airy beams," *IEEE Photon. J.*, vol. 9, no. 1, Feb. 2017, Art. no. 6500510.
[20] G. A. Siviloglou, J. Broky, A. Dogariu, and D. N. Christodoulides, "Observation of accelerating Airy beams," *Phys. Rev. Lett.*, vol. 99, no. 21, Nov. 2007, Art. no. 213901.
[21] G. A. Siviloglou, J. Broky, A. Dogariu, and D. N. Christodoulides, "Ballistic dynamics of Airy beams," *Opt. Lett.*, vol. 33, no. 3, pp. 207–209, Feb. 2008.
[22] A. Chong, W. H. Renninger, D. N. Christodoulides, and F. W. Wise, "Airy-Bessel wave packets as versatile linear light bullets," *Nature Photon.*, vol. 4, no. 2, pp. 103–106, Jan. 2010.
[23] P. Polynkin, M. Kolesik, J. V. Moloney, G. A. Siviloglou, and D. N. Christodoulides, "Curved plasma channel generation using ultraintense Airy beams," *Science*, vol. 324, no. 5924, pp. 229–232, Apr. 2009.
[24] Y. Qian and S. Zhang, "Quasi-Airy beams along tunable propagation trajectories and directions," *Opt. Exp.*, vol. 24, no. 9, pp. 9489–9500, Apr. 2016.